Chemistry–A European Journal
Research Article
doi.org/10.1002/chem.202401833
Chemistry Europe
European Chemical Societies Publishing
www.chemeurj.org

Synthesis of Asymmetric Ionic Hybrid Detergents enables Micelles with Scalable Properties including Cell Compatibility

Virginia Wycisk,*[a] Jan-Simon Behnke+,[a] Lena Nielinger+,[a] Marc Seewald+,[a] Jörn Weisner,[a] Markus Binsch,[a] Marc-Christian Wagner,[a] Tobias Raisch,[b] and Leonhard H. Urner*[a]

Ionic detergents enable applications and cause harm in biospheres due to cell toxicity. The utility of covalent combinations between ionic and non-ionic detergent headgroups in modulating cell toxicity remains speculative due to the yet rarely explored synthesis. We close this gap and establish the modular synthesis of ionic/non-ionic hybrid detergents. We restructure a combinatorial methallyl dichloride one-pot coupling into a two-step coupling, which reduces by-products, improves product yields, and enables the gram-scale preparation of asymmetric, cationic/non-ionic and anionic/non-ionic hybrid detergents. Our modular synthesis delivers new modalities for the design of ionic detergents, including an unprecedented scaling of properties that determine applications, such as charge, critical micelle concentration, solubilizing properties, hard water tolerance, and cell compatibility. We uncover that shielding the charge in ionic headgroups can switch the detergent species that is toxic to cells from monomers to mixtures of monomers and micellar assemblies. Establishing the chemistry of ionic/non-ionic hybrid detergents provides a missing evolutionary link in the structural comparison of ionic and non-ionic detergents, enables an easy synthesis access to yet unexplored chemical spaces of asymmetric hybrid materials, and delivers new modalities for designing the toxicity of supramolecular nanomaterials.

Introduction

Ionic and non-ionic detergents enable fundamental applications in industry, households, and academia.[1] The simple molecular structure of detergents consists of a polar head and a non-polar tail. According to the charge of the headgroup, the detergentome is divided into three detergent classes, i.e., cationic, anionic, non-ionic (Scheme 1).[1f] To reduce development costs and the ecological foot print of detergent products, design guidelines are needed to predictably optimize molecular structures and mixtures for applications.[1f,2] The implementation of structure-property studies to deliver design guidelines is a challenge. When comparing different detergent classes, more than one structural parameter changes at once, including structural arrangement and charge, which makes it difficult to run conclusive structure-property studies (Scheme 1).[3]

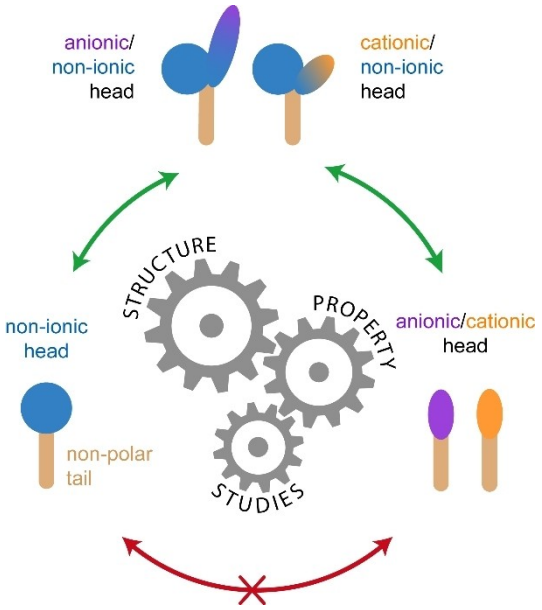

Scheme 1. Ionic and non-ionic detergents are difficult to compare. Ionic/non-ionic hybrid detergents are established to provide an evolutionary link between the two chemical spaces of non-ionic and ionic detergents.

The era of synthetic detergent chemistry recently surpassed its 100th anniversary.[1a] Due to increasing production and disposal volumes, interactions between ionic detergents with human cells and bacteria become increasingly relevant, for example, in context with laundry, personal hygiene, or contaminations of aquatic ecosystems.[1c–e,4] Chronic exposure to detergents is associated with inflammatory responses in

[a] V. Wycisk, J.-S. Behnke,+ L. Nielinger,+ M. Seewald,+ J. Weisner, M. Binsch, M.-C. Wagner, L. H. Urner
TU Dortmund University, Department of Chemistry and Chemical Biology, Otto-Hahn-Str. 6, 44227 Dortmund
E-mail: virginia.wycisk@tu-dortmund.de
leonhard.urner@tu-dortmund.de
[b] T. Raisch
Max Planck Institute of Molecular Physiology, Department of Structural Biochemistry, Otto-Hahn-Str. 11, 44227 Dortmund
[+] these authors contributed equally

Supporting information for this article is available on the WWW under https://doi.org/10.1002/chem.202401833

mammalian cells and changes in antibiotic resistance profiles in microbial communities.[5] The chemistry of detergents that serves the purpose of applications without harming cells is becoming increasingly relevant and needs to be explored.[4]

Cell toxicities of detergents are linked to the chemical nature of ionic headgroups. Cationic detergents, like dodecyl trimethyl ammonium bromide (DTAB), can be used as disinfectants or fabric softeners.[1c,d,2] They have millimolar critical micelle concentration (cmc) values, good hard water tolerances, moderate solubilizing properties, and high cell toxicities.[1c,d,6] Anionic detergents, like sodium dodecyl sulphate (SDS), are used in domestic cleaning products and have millimolar cmc values, poorer hard water tolerances, moderate solubilizing properties, and are less cell toxic than cationic detergents.[1e,6] Ionic detergents are optimized by changing the structure of ionic groups[1f,g] or non-polar tails.[1f,g] We expect fusing non-ionic and ionic headgroups covalently will allow shielding the charge of a detergent head and deliver a complementary modality for tuning the cell toxicity of detergents. Furthermore, depending on the concentration, detergents can be present as monomers or mixtures of monomers and micellar assemblies. Whether the ionic detergent species toxic to cells are detergent monomers or mixtures of monomers and aggregates has not been fully addressed.[4] Our systematically designed set of ionic detergents and ionic/non-ionic hybrid detergents will help to clarify the relation between detergent structure, toxic species, and cell toxicity.

Several prototypes of ionic/non-ionic hybrid detergents have been established, e.g., rhamnolipids,[7] glucosyl-substituted dicarboxylate detergents,[8] gluco-pyridinium surfactants,[9] and glucocationic surfactants.[10] To discover the potential of hybrid detergents in modulating cell toxicity, herein, we establish a modular synthesis of asymmetric ionic/non-ionic hybrid detergents. Subsequently, we harness the structural scalability of ionic/non-ionic hybrid detergents to investigate how changes in the relative molecular weight fraction of ionic groups modulate detergent properties relevant for cell toxicity, including ionic character, cmc, solubilization properties, and hard water stability.

Results and Discussion

Synthesis of Asymmetric Detergents

To enable the synthesis of ionic/non-ionic hybrid detergents, we harnessed an asymmetric methallyl dichloride coupling strategy.[3] Initially, the Haag lab established this approach for the preparation of symmetric, acetal-protected oligoglycerol dendrons.[11] More lately, the Urner lab brought this approach further to enable the preparation of asymmetric, non-ionic hybrid detergents in a combinatorial synthesis approach.[3,12] The key observation to this development was that a reaction of two non-ionic headgroup precursors (**a**, **b**) with methallyl dichloride under SN2' conditions in one pot can lead to a trimeric headgroup mixture (**aa**, **ab**, **bb**) (Figure 1A).[3,12] Here, we restructured this concept to an asymmetric two-step approach to enable the synthesis of ionic/non-ionic hybrid detergents.

As starting materials, we selected non-ionic headgroup precursors with orthogonal protecting groups, i.e., acetal-protected solketal (**pG0**), acetal-protected triglycerol (**pG1**), and benzyl-protected ethylene glycol (**BnO-E1**) (Figure 1A). Following a combinatorial one-pot coupling, three products were obtained (**aa**, **ab**, **bb**) which could be isolated by normal-phase chromatography (Figure 1A). Regardless of the starting material combinations, e.g., **pG0** and **BnO-E1** or **pG1** and **BnO-E1**, similar yields were obtained for individual products, which consolidates the robustness of this approach (Figure 1A).[3] Previous results showed that the combinatorial one-pot coupling can be used to accelerate the diversity-oriented preparation of non-ionic detergent headgroups.[3] However, we expect the economic potential of this combinatorial coupling is limited if the desired product is only the asymmetric compound **ab**. Two by-products are formed in substantial yields, e.g., **aa** and **bb**, which limits obtainable yields of the desired compound **ab** (Figure 1A).

To optimize the yield of the desired asymmetric product **ab**, we divided the methallyl dichloride coupling into two synthesis steps (Figure 1A). First, **pG0** (**a**) was reacted with equimolar amounts of methallyl dichloride to obtain the monosubstituted intermediate **a*** (Figure 1A). Second, **Bn-OE1** (**b**) was reacted with the monosubstituted intermediate **a*** to obtain the desired product **ab** (Figure 1A). Even though the two-step approach required two purification steps, the by-product **bb** was eliminated, and the yield of **ab** increased to 50% (Figure 1A). Furthermore, less starting material was required during the second step to finalize the asymmetric detergent headgroup precursor **ab** compared to the combinatorial one-pot coupling. Our two-step approach can save starting material for the benefit of product yields, which can be beneficial, especially, if one of the detergent headgroup precursors is difficult to synthesize (Figure 1A). In addition, the asymmetric intermediate **a*** can be produced in gram scale and is stable at 4 °C under normal atmosphere for long-term storage (> 6 month) (Figure 1A). Designing asymmetric compounds in high yields is a common challenge in organic chemistry.[12–13] Our two-step coupling strategy will facilitate the preparation of asymmetric modular architectures beyond this work.

Having established the synthesis of the asymmetric headgroup **ab**, the synthesis of ionic/non-ionic detergent precursors **1** and **2** was accomplished in four steps, i.e., ozonolysis, reduction, alkylation, hydrogenolysis (Figure 1B). Modularity is key to scalability of structure, properties, and function.[11,14] An established example are dendrimers, which contain a scalable number of functional groups at the periphery and a single chemically addressable functional group at the focal point.[15] Encouraged by the fact that the hybrid detergent precursors **1** and **2** contain an independently addressable hydroxyl group, we established its utility for modular chemistry by successfully employing standard coupling reactions, i.e., mesylation,[11] azidation,[11] reductive amination,[11] Appel reaction,[16] propargylation,[12] copper-catalyzed triazole formation,[17] N- and O-alkylation, including sultone addition and quaternization (Figure 1C).[18]

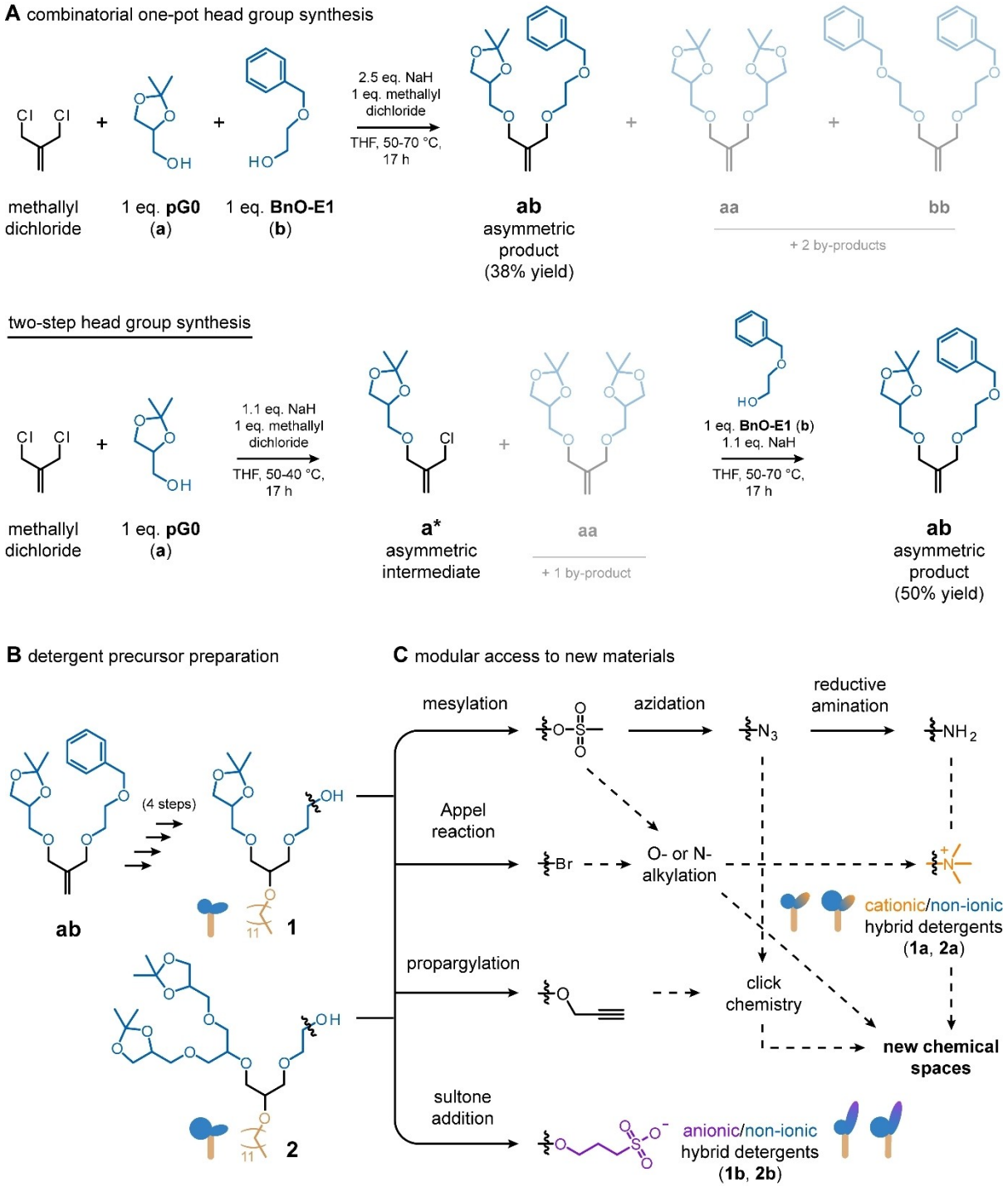

Figure 1. Overview of key steps in the preparation of ionic/non-ionic hybrid detergents. (A) Schematic showing that restructuring the detergent headgroup preparation from a combinatorial one-pot synthesis into a two-step synthesis reduces by-products and increases yields of asymmetric headgroup precursors (**ab**). (B) Schematic showing that a conversion of **ab** can deliver asymmetric detergent precursors with independently addressable hydroxyl groups (**1**, **2**). (C) Overview of chemical transformations that can be applied to the independently addressable hydroxyl groups in **1** and **2** to obtain charged hybrid detergents (**1a**, **2a**, **1b**, **2b**). The underlying modular chemistry provides an access to chemical spaces beyond this project.

The latter functionalization strategies in combination with a removal of acetal protecting groups led to cationic/non-ionic hybrid detergents (**1a**, **2a**), and anionic/non-ionic hybrid detergents (**1b**, **2b**) (Figure 1C) (Figure 2B). The two-step synthesis option of methallyl dichloride coupling in conjunction with modular chemistry enables the fusion of ionic and non-ionic detergent headgroups into hybrid detergents with unbeatable ease. The capability of our modular chemistry to change functionality in detergents with well-established reactions in gram scale will facilitate structure-property studies.

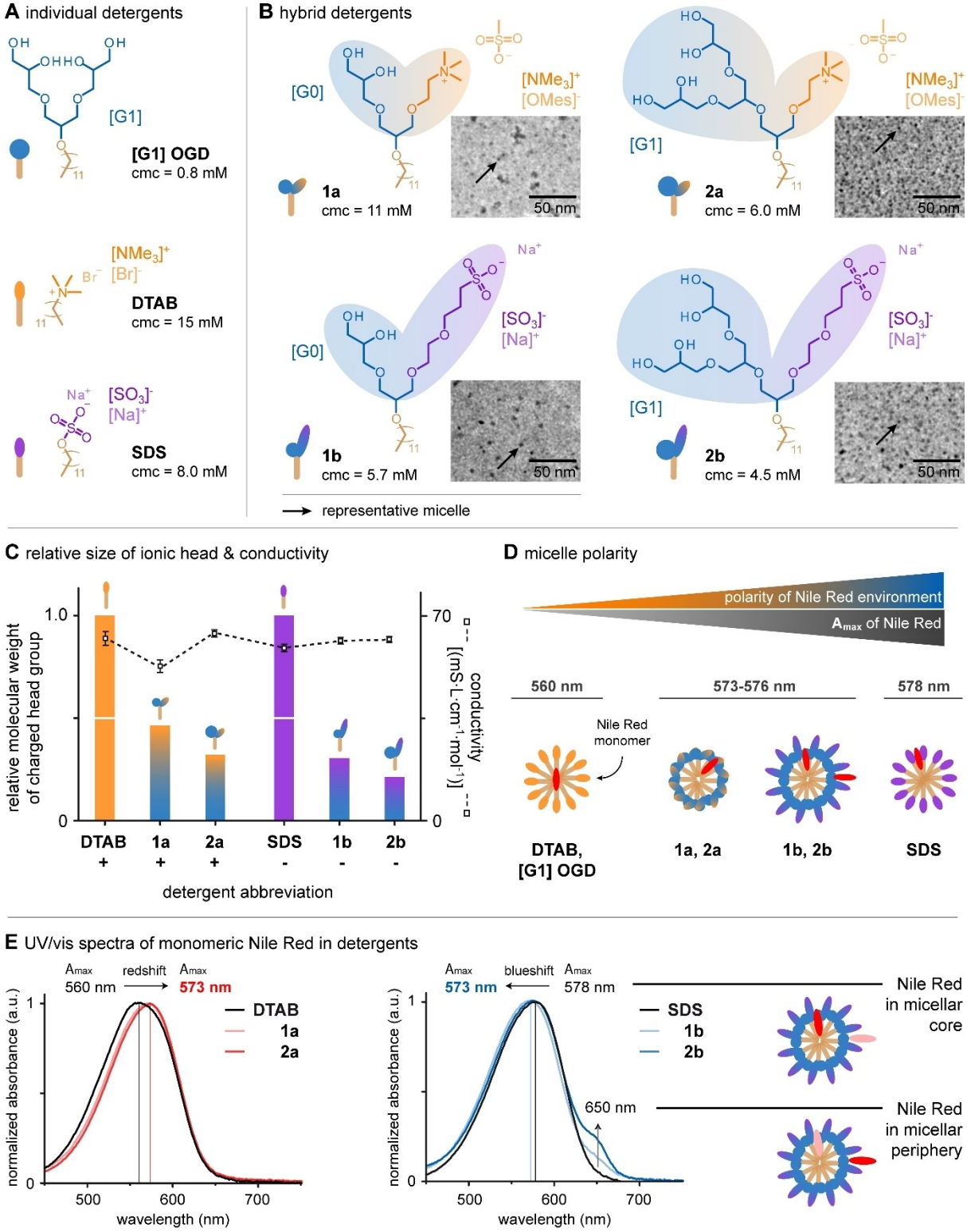

Figure 2. Molecular and supramolecular properties of ionic hybrid detergents. (A) Molecular structures of parent detergents and (B) related hybrid detergents, including cryo-EM images of their micelles in water and cmc values. (C) Bar chart showing the relative molecular weight fractions of charged headgroups in detergents and molar conductivities. (D) Schematic highlighting the localization and relative polarity of the environment surrounding Nile Red in detergent micelles. Structure of micelles shown as cartoons may differ from solution structures. (E) UV/Vis spectra of monomeric Nile Red in aqueous detergent solutions and schematics highlighting possible localizations of the dye in micelles formed by anionic hybrids (**1 b**, **2 b**).

Scalable Molecular and Supramolecular Properties

Detergent properties, like ionic character and cmc values, determine applications and cell toxicity (Figure 2A–B).[1c–e,2, 19] Since we installed a non-ionic group in proximity to ionic headgroups, we asked whether the ionic character and charge-repulsive interactions between ionic/non-ionic detergent monomers are similar to their parent detergents. To better compare the impact of headgroup structures on both variables, we plotted the relative molecular weight fraction of ionic groups against the detergent abbreviation and compared those values with conductivities and cmc values (Figure 2C).

The relative molecular weight fraction of the ionic head with respect to the complete headgroup, such as in the cases of DTAB and SDS, got reduced to ~38% and ~27% after adding non-ionic glycerol and triglycerol, respectively (Figure 2C). However, molar conductivity values obtained from ionic/non-ionic hybrid detergents (**1a**, **2a**, **1b**, **2b**), DTAB, and SDS scatter around a value of 60 (Figure 2C). Decreasing the relative molecular weight fraction of ionic headgroups did not noticeably affect the ionic character of hybrid detergents (Figure 2C).

We hypothesized that decreasing the relative molecular weight fraction of ionic headgroups reflects a better shielding of the charge, which reduces repulsive detergent-detergent interactions. Ionic/non-ionic hybrid detergents formed micellar assemblies with average diameters not bigger than 5 nm and cmc values between 4.5 mM and 11 mM (Figure 2A–B) (Figure S1). Electrostatics are among the strongest forces available to modulate intermolecular interactions in nature.[20] A better shielding of charged headgroups should reduce electrostatic repulsion between detergent monomers thereby reducing the cmc.[21] However, DTAB, SDS, and related hybrid detergents (**1a**, **2a**, **1b**, **2b**) are difficult to systematically compare, because the chemical nature of charged groups also plays a role in cmc. For example, the DTAB cation has a bigger hydration shell compared to the SDS anion.[22] The distance between DTAB cation and counterion is larger compared to SDS.[22] The charge of the DTAB cation is less efficiently shielded by counterions, which enhances electrostatic repulsion between detergent monomers and is reflected in an almost two-fold increase in cmc compared to SDS (Figure 2A).[22] Furthermore, the structures of our hybrid detergents are not directly comparable. The linkers between charged headgroups and non-polar tails in cationic/non-ionic hybrid detergents (**1a**, **2a**) are shorter compared to anionic/non-ionic hybrid detergents (**1b**, **2b**). Repulsive electrostatic interactions between equally charged headgroups are enhanced when the distance between polar groups and non-polar tail is reduced.[23] Therefore, higher cmc values were obtained in the cases of cationic/non-ionic hybrid detergents (**1a**, **2a**) compared to anionic/non-ionic hybrid detergents (**1b**, **2b**) (Figure 2B).

Considering differences in charged headgroups and distances between charged headgroups and non-polar tails, we compared our anionic and cationic detergent series separately. We observed consistently a reduction in cmc values within our positively charged (DTAB, **1a**, **2a**) and negatively charged detergent series (SDS, **1b**, **2b**), respectively (Figure 2A–B). In line with our hypothesis, repulsive electrostatic interactions between hybrid detergent monomers were reduced compared to ionic parent detergents, and the aggregation tendency was increased, as reflected by lower cmc values (Figure 2A–B). In addition to a better shielding of charged headgroups, non-ionic glycerol and triglycerol are amphiphilic building blocks that add polar hydroxyl groups as well as non-polar ether groups. The decrease in cmc is likely also supported by a relative decrease in overall detergent polarity caused by the extension of the non-polar ether backbone from glycerol to triglycerol, respectively (Figure 2A–B).[24] Fusing ionic and non-ionic headgroups delivered a strategy for the design of ionic/non-ionic hybrid detergents with lower cmc values compared to the related cationic DTAB and anionic SDS, from a modular chemistry perspective (Figure 2A–B).

Seen from a broader perspective, the cmc is an important design criterion for all supramolecular materials.[19c] Modulating the balance between ionic and non-ionic headgroups delivers a new direction for the design of detergents with customizable cmc values in proteomics,[19d,25] membrane protein structural biology,[1b,26] and laundry applications.[2] The cmc of ionic detergents can be tuned by varying the length of the hydrocarbon tail,[27] the preparation of detergent mixtures,[2,28] or by varying the salt concentration in solution.[27a,29] Our work complements design strategies by enabling a modulation of cmc by scaling the relative size of the non-ionic head in hybrid detergents. The concept of hybrid detergents will transform the scalability of charged supramolecular materials.

Charge Distance and Backbone Size Determine Guest Localization

In aqueous solution, micelles are in dynamic exchange with detergent monomers and oligomers, thus enabling the encapsulation and release of hydrophobic matter.[1f,19c,30] This includes non-polar guest molecules relevant to the modulation of cell toxicity, like drugs, lipids, and membrane proteins. To understand the role of detergent headgroup combinations in solubilizing hydrophobic molecules, we doped the micelles obtained from ionic/non-ionic hybrid detergents and reference detergents with low concentrations of the water-insoluble dye Nile Red (10 μg/mL).[31] Under the chosen experimental conditions, Nile Red is solubilized in monomeric form and the wavelength of the absorbance maximum informs on the polarity of its surrounding micellar environment (Figure 2D–E).[11,31–32]

Our data show that the localization of Nile Red in micellar environments can be gradually modulated by changing the chemical nature of detergent headgroups (Figure 2D–E). Specifically, Nile Red encapsulated in anionic hybrid detergents (**1b**, **2b**) showed a blue shift in comparison to SDS, while in cationic hybrid detergents (**1a**, **2a**) a red shift was obtained in comparison to DTAB (Figure 2D–E).

The polarity of micellar environments provided by SDS and DTAB are different and shifts in absorption obtained from

related hybrid detergents are discussed separately. In the cases of DTAB and cationic hybrid detergents (**1a**, **2a**), we expect the polyether backbones of non-ionic headgroups represent a less hydrophobic extension of the non-polar alkyl tails, which can also interact with the Nile Red surface during encapsulation.[11] However, we expect the positive charge adjacent to the non-ionic polyether backbones increased the polarity in this environment (Figure 2B), which forces hydrophobic Nile Red to insert more deeply into the micellar core compared to anionic hybrid detergents (**1b**, **2b**). The micellar environment provided by cationic hybrid detergents (**1a**, **2a**) is more polar compared to DTAB (Figure 2D–E). In the cases of anionic hybrid detergents (**1b**, **2b**), the negative charge is more adjacent to the free hydroxyl groups of the non-ionic headgroups (Figure 2B). We expect this forces hydrophobic Nile Red to insert less deeply into the micellar core compared to anionic SDS as indicated by a blue shift in absorption (Figure 2D–E). The ability to tune the size of the polyether backbone and proximity to charge in ionic/non-ionic hybrid detergents offers a new modality for tuning the localization of hydrophobic guest molecules in micelles, including the polarity of the surrounding host environment.

Surprisingly, only in the cases of anionic/non-ionic hybrid detergents (**1b**, **2b**), the UV/Vis spectra of solubilized Nile Red showed two absorbance maxima at 573–576 nm and 650 nm (Figure 2E). The absorbance maxima at lower wavelengths, i.e., 573–576 nm, are characteristic for Nile Red embedded within micelles near the hydrophobic core (Figure 2E).[31] In contrast, the absorbance maximum at 650 nm is characteristic for monomeric Nile Red whose environment is as polar as water.[33] However, control experiments confirmed that Nile Red cannot be solubilized in monomeric form in detergent-free water under the chosen experimental conditions.[32] We conclude that anionic/non-ionic hybrid detergents (**1b**, **2b**) provide a micellar environment in which Nile Red monomers can localize not only within the micellar core near the non-polar alkyl tails but also within the polar periphery of the micelles (Figure 2E).[31–32] We did not observe an absorbance maximum at 650 nm in the cases of cationic hybrid detergents (Figure 2E). This indicates that the length of the linker between charge and tail determines the ability to encapsulate Nile Red in the polar periphery of ionic/non-ionic hybrid detergent micelles.

The ability to control the localization of hydrophobic guest molecules in detergent micelles has important implications for drug discovery. The localization of hydrophobic and pharmaceutically active ingredients in micellar drug formulations can alter biological activity.[34] However, drug localization in solubilizing agents is difficult to control, hence their role in modulating biological function is rarely understood.[34] The ability to gradually shift the localization of encapsulated guest molecules from micelle core to micelle periphery by changing ionic/non-ionic hybrid detergent headgroups delivers a starting point for the development of micellar nanocarriers with controllable guest localization (Figure 2D). The current weakness of our conclusion is that we could not transfer the principle of controllable guest localization in the micelles obtained for Nile Red to other drug molecules. As controls, we included the poorly water-soluble chemotherapeutic dipyridamole and the better water-soluble chemotherapeutic doxorubicin (non-hydrochloride). We observed similar spectral shifts in all detergents in the cases of doxorubicin and dipyridamole (Figure S2). This underlines that solubilizing properties depend on both the structure of detergent and hydrophobic guest.[34c]

Charge Determines Micelle Solubilization Efficiency

Detergent micelles are commonly applied to improve water solubility of hydrophobic compounds in applications, like drug solubilization, membrane protein research, and laundry.[1f,30,34c] The solubilization of hydrophobic lipids in detergent-cell interactions is linked to membrane damage, which contributes to cell toxicity.[4] To design detergents as solubility promoting agents with low cell toxicities, it is interesting to control the solubilization efficiency of detergents.[34c] To establish the potential of ionic/non-ionic hybrid detergents in controlling the solubilization efficiency of micelles in water, we investigated how much Nile Red can be solubilized with detergents by using the film uptake method.[35] To account for the fact that comparable aggregate concentrations are provided in solution, Nile Red was solubilized at detergent concentrations of 2x cmc.[30]

In terms of absolute Nile Red quantities that were solubilized under the employed experimental conditions, the cationic/non-ionic hybrid detergent **1a** performed best (Figure 3A). Intermediate Nile Red quantities were solubilized by cationic DTAB, anionic SDS, and the anionic/non-ionic hybrid detergent **1b** (Figure 3A). Fusing ionic detergents headgroups with small non-ionic detergents headgroups, like glycerol, delivered a strategy to design ionic detergents with good solubilizing properties. Furthermore, lower Nile Red quantities were solubilized in the cases of non-ionic [G1] OGD and hybrid detergents containing a larger non-ionic headgroup, i.e., triglycerol (**2a**, **2b**) (Figure 3A). Increasing the size of the non-ionic headgroup in ionic/non-ionic headgroups delivered a strategy to down-regulate the solubilizing properties of ionic/non-ionic hybrid detergents.

Due to the different cmc values, the absolute Nile Red quantities that were encapsulated by the detergents at 2x cmc did not directly inform on solubilization efficiency (Figure 3A). To better assess how the solubilization efficiencies of the detergents were modulated by the structure of the headgroups, we plotted the molar amounts of Nile Red that got solubilized per molar amount of detergent (Figure 3B). Our data confirmed that the characteristic solubilization efficiencies of non-ionic and ionic detergent headgroups are retained, regardless of whether ionic headgroups were fused with non-ionic headgroups.[2,30,36] Owing to its lower cmc, the highest solubilization efficiency was obtained for non-ionic [G1] OGD (Figure 3A).[2,30] Moderate solubilization efficiencies were obtained for anionic and cationic detergents (SDS, **1b**, **2b**, DTAB, **1a**, **2a**)

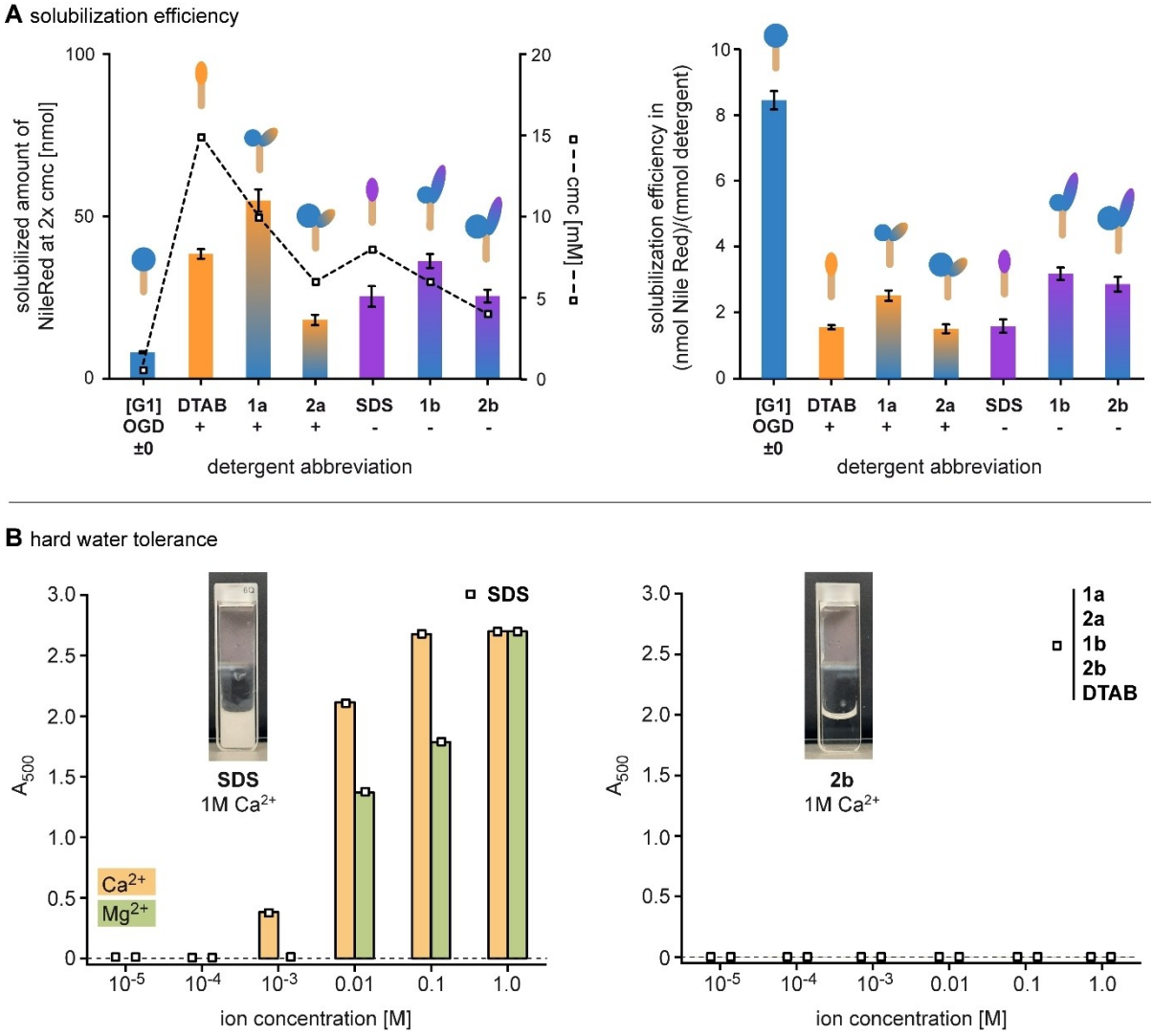

Figure 3. Detergent structure affects solubilization efficiency and hard water tolerance. A) Bar charts showing the amount of Nile Red solubilized in water by detergents at 2x cmc (left graph) and solubilization efficiency expressed in molar amount of Nile Red solubilized per molar amount of detergent. Higher relative solubilization efficiencies were obtained from non-ionic [G1] OGD and ionic/non-ionic hybrid detergents containing a smaller non-ionic glycerol head (**1a**, **1b**). B) Bar charts showing absorbance values at 500 nm (A500) obtained from aqueous detergent samples at 4x cmc of SDS (left) and other detergents (DTAB, **1a**, **2a**, **1b**, **2b**) (right) in the presence of different calcium and magnesium ion concentrations. Cationic DTAB as well as ionic/non-ionic hybrid detergents (**1a**, **2a**, **1b**, **2b**) are more resistant against precipitation in the presence of divalent cations than anionic SDS. Source data for the bar charts are provided in the Electronic Supporting Information (Table S1–2).

(Figure 3A).[2,30] We observed similar trends for dipyridamole, which consolidated the hypothesis that charged headgroups downregulate the solubilization efficiency of detergents compared to non-ionic headgroups (Figure S3).[2,30]

The ability to up- or downregulate the solubilizing properties of detergents is key to successful structure-property studies and applications in various research fields, including proteomics,[19d,25] drug delivery,[19b,37] and the development of cleaning products.[2,38] Another important aspect of detergent micelles in these research areas is their resistance against precipitation in the presence of divalent cations which are often present in biological assays.[39]

Anionic detergents are prone to precipitate in the presence of divalent cations, like magnesium and calcium, which can diminish their utility as solubilizing agents.[40] To understand whether fusing non-ionic and ionic headgroups affects precipitation resistance, we tracked the turbidity of detergent solutions at 4x cmc at 500 nm by UV/Vis spectroscopy against magnesium and calcium ion concentrations (Figure 3B).[40b] SDS was used as positive control as it readily precipitates in the presence of divalent cations. DTAB was used as negative control.[40b]

Our data confirmed the precipitation susceptibility of SDS micelles. An increase in sample turbidity was obtained in the presence of calcium and magnesium ion concentrations of 1 mM and 10 mM, respectively (Figure 3B). In contrast, no increase in sample turbidity and precipitation was obtained in the cases of DTAB and the ionic/non-ionic hybrid detergents (**1a**, **2a**, **1b**, **2b**) for divalent ion concentrations up to 1 M (Figure 3B). Anionic detergents, like SDS, can precipitate in the

presence of magnesium and calcium, because attractive charge interactions between anionic detergent headgroups and divalent cations enable the formation of water-insoluble aggregates.[40] Specifically, in the cases of anionic/non-ionic hybrid detergents, we expect the non-ionic headgroups shield the negatively charged headgroups, which inhibits the formation of water-insoluble detergent-salt aggregates. Fusing ionic and non-ionic headgroups enables the design of detergents that are intrinsically resistant against precipitation in hard water, which enables the investigation of detergent interactions with cells in biological assays.

Ionic hybrid Detergents Exhibit Scalable Cell Compatibility

Detergents are commonly in contact with living matter. Every day examples are related to the use of detergents in household applications and include microbiome-detergent interactions on textiles,[41] oral uptake through food contaminations,[5d] or the inhalation through shampoo aerosols.[1e] Similar to cmc, encapsulation efficiency, and hard water tolerance, the charge of the detergent head determines cell compatibility.[6,42] Owing to their electrostatic nature, purely ionic detergents exhibit rather harsh properties, suggesting a need for milder alternatives.[1e,43] Here, we establish the potential of ionic/non-ionic hybrid detergents to deliver a new modality for tuning cell compatibility.

Testing the toxicity of detergent molecules on the cellular level *in vitro* is a standard approach to assess the harmful potential for biological systems.[42a] To investigate how combining headgroups of ionic and non-ionic detergents affects cell toxicity, we chose established *in vitro* reference systems, i.e., the spontaneously immortalized keratinocyte HaCaT cell line as human model and *E. coli* MG1655 as bacterial model.[42a,44] Monitoring cellular growth of HaCaT cells in our cell viability assay delivered the concentrations at which detergents exert half of their maximal growth inhibitory effect (IC_{50}). Monitoring bacterial growth using the broth microdilution assay delivered the minimal inhibitory concentration at which bacterial growth was fully diminished (MIC).[45]

Our experiments showed that cell compatibility of ionic/non-ionic hybrid detergents depends on four parameters, i.e., the charge of the head (positive or negative), the relative size of the non-ionic headgroup, cmc values, and cell line.[4,6] The charge of the head determines the ease of detergent insertion into membranes. Cell membranes are the first point of contact between cells and detergents. The insertion of detergent monomers into membranes induces membrane damage and leads to cell death.[4] Outer membranes of Gram-negative bacteria, like *E. coli*, and cytoplasmic membranes of mammalian cells, like HaCaTs, have net negative surface potentials.[46] Membranes are intrinsically more repellent to anionic detergents compared to positively charged detergents due to repulsive electrostatic interactions. Therefore, anionic detergents have higher IC_{50} and MIC values compared to cationic detergents under the experimental conditions employed (Table 1).[6]

Table 1. Cell toxicity data. Overview of detergents (detergents), charge (charge), critical micelle concentration (cmc), IC_{50} values for mammalian HaCaT cells (IC_{50}) as well as MIC values for *E. coli* MG1655 (MIC). Data are shown with standard deviation (±SD) from three independent biological repeats (n = 3). Highest possible concentrations tested for **1 b** and **2 b** were determined by the solubility limit and are labelled with an asterisk.

detergent	charge	cmc/mM	IC_{50}/μM (HaCaT)	MIC/mM (*E. coli*)
[G1] OGD	±0	0.80	49 ± 5	> 290
DTAB	+	15	3 ± 1	0.30
1 a	+	11	3 ± 1	0.30
2 a	+	6.0	17 ± 2	1.00
SDS	–	8.0	278 ± 65	290
1 b	–	5.7	366 ± 94	> 290*
2 b	–	4.5	4382 ± 1769	290*

Regardless of the cell line, IC_{50} and MIC values of cationic detergents (DTAB, **1 a**, **2 a**) were well below their cmc values, suggesting detergent monomers to be the toxic species (Table 1). IC_{50} and MIC values of cationic detergents can be readily reduced by increasing the relative size of the non-ionic headgroup. We conclude that increasing the relative size of the non-ionic headgroup decreases attractive electrostatic detergent-membrane interactions and cell toxicities in the direction from DTAB and **1 a** to **2 a** (Table 1) (Figure 4).

In contrast, trends in cell toxicities obtained from anionic detergents (SDS, **1 b**, **2 b**) varied with the cell line. For mammalian HaCaT cells, IC_{50} values of SDS and **1 b** were below their cmc values, suggesting again detergent monomers to be the toxic species (Table 1). Surprisingly, shielding the charge in **1 b** further by installing a triglycerol head in **2 b** led to IC_{50} values that were similar to the detergent's cmc value (Table 1). This suggests that the cell toxicity of **2 b** is no longer solely linked to detergent monomers but also to the presence of micelles (Figure 4). Detergent micelles will likely follow a different mode of action in membrane interaction compared to detergent monomers. Depending on the concentration, detergent monomers insert into membranes and induce a phase transition that can culminate in complete membranolysis.[47] Micelles likely collide with membranes and increase the detergent concentration locally, which can induce partial membrane lysis, pore formation, and cell death.[48] We expect that shielding the charge of the anionic head in **2 b** by adding non-ionic triglycerol makes its negatively charged micellar assemblies less repellent to membranes compared to **SDS** and **1 a** (Figure 4).

This explanation nicely agrees with the unusual trend in MIC values obtained for *E. coli* (Table 1). The MIC values of SDS, **1 a**, and **2 b** were all above the detergents' cmc values (Table 1). Unlike mammalian cells, Gram-negative bacteria, like *E. coli*, contain a peptidoglycan layer that is surrounded by two lipid membranes.[49] This triple layered membrane architecture makes Gram-negative bacteria more resistant against detergent monomers, which is reflected in higher concentrations required to induce cell death compared to HaCaT cells (Table 1). Since the

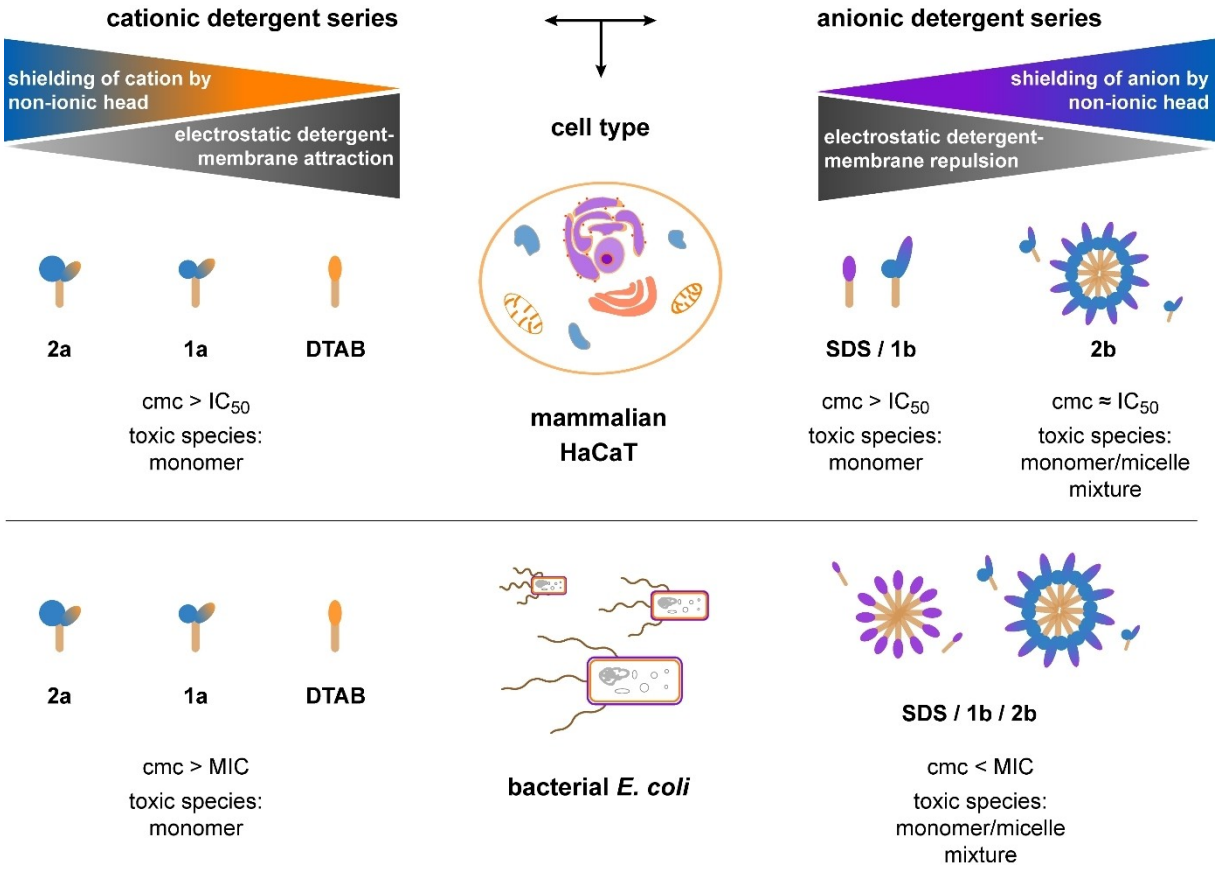

Figure 4. Analysis of the toxic detergent species. Schematic that qualitatively compares the impact of detergent charge (cation, anionic), cell type (HaCaT, *E. coli*), cmc, IC_{50} values, and MIC values to propose the toxic detergent species. Depending on charge, shielding of the charge, cmc, and cell type, the toxic detergent species switches between monomers and mixtures of monomers and aggregates.

toxicity of our anionic detergents is linked to the presence of micellar assemblies, we expect that shielding the anionic charge by increasing the size of the non-ionic headgroup reduced repulsive detergent-membrane and micelle-membrane interactions, which promoted membrane damage and cell death (Figure 4). Therefore, we observed lower MIC values in the case of **2 b** compared to **1 b** (Table 1).

Conclusions

In summary, our results complement the view that ionic detergent monomers are the only possible species toxic to cells.[47b] We show that shielding the charge in ionic/non-ionic hybrid detergents can switch the toxic detergent species from monomers to mixtures of monomers and micellar assemblies. To investigate the molecular underpinning, we established the facile synthesis of ionic/non-ionic hybrid detergents and established a two-step methallyl dichloride coupling that increases asymmetric product yields. Ionic/non-ionic hybrid detergents represent a new class of detergents that form micellar assemblies and whose supramolecular properties depend on the charge of the ionic detergent head, distance between ionic head and non-polar tail, and relative size of the non-ionic head. Installing a non-ionic headgroup near a charged headgroup reduces repulsive intermolecular detergent-detergent interactions and cmc values. Micellar assemblies formed by ionic/non-ionic hybrid detergents exhibit good solubilization efficiencies compared to ionic standards SDS and DTAB, are intrinsically resistant against precipitation in the presence of divalent cations and deliver a starting point for controlling the localization and polarity of the micellar environment surrounding encapsulated guest molecules.

Furthermore, varying the shielding of the charge in ionic/non-ionic hybrid detergents delivered a modality to modulate cell toxicity. Our data indicate that cell toxicities of cationic detergents are strictly linked to their monomers because of attractive electrostatic detergent-membrane interactions that drive membrane damage and cell death. Anionic detergents have lower cell toxicities as they are more repellent to membranes due to repulsive electrostatic detergent-membrane interactions. Depending on the cell type, the toxic species of anionic detergents can switch from monomers to mixtures of monomers and micellar assemblies. More fragile mammalian skin cells are more susceptible to anionic detergent monomers compared to more robust Gram-negative bacteria, which are only susceptible to mixtures of anionic detergent monomers and micellar assemblies. Our data indicate that shielding the negative charge of the headgroup in hybrid detergents through non-ionic triglycerol reduces repulsive electrostatic interactions

between their micellar assemblies and membranes which increases toxicity against Gram-negative *E. coli*. Our findings uncovered a new detergent chemistry which enables tuning the cell toxicities of detergent monomers and micellar assemblies, from a supramolecular chemistry perspective. Ionic/non-ionic hybrid detergents outline new possibilities for the design of supramolecular nanomaterials with customizable cell toxicities for future applications.

Experimental Section

Starting Materials for Detergent Synthesis

General information about chemicals, purification workflows, and compound characterization were adopted as previously described: Chemicals were purchased from Sigma-Aldrich (Germany), Acros Organics (Germany), Alfa Aesar (Germany), Fluka (Germany), Fischer Scientific (Germany), Merck (Germany), and were used as supplied. Solvents were used as supplied. Dry solvents were purchased in bottles that were sealed with a septum and kept under inert atmosphere. Deionized water (H_2O) for synthesis was taken from a PURELAB flex system (LC134, Veolia Water Technologies, Germany) whose water supply was obtained from a water deionization system installed at TU Dortmund University. Argon and oxygen were purchased from Linde (Germany) and used as supplied. For working under dry and oxygen-free reactions conditions, chemicals and solvents were handled under argon atmosphere.

General Information for Detergent Purification and Characterization

For reaction monitoring and purification procedures, normal phase (NP) thin-layer chromatography (TLC) analysis was applied. NP TLC plates (DC-Fertigfolien ALUGRAM® Xtra SIL G/UV254) based on silica (SiO_2) were purchased from Macherey-Nagel (Germany). Silica gel (60 M) for preparative normal phase column chromatography was purchased from Macherey-Nagel. For NP TLC analysis and manual NP column purification mixtures of organic solvents (v:v) were prepared. If necessary, methanol or ethyl acetate was added in percent per volume to the prepared mixtures (v:v + v%). TLC plates were either analyzed under UV light (254 nm) or by staining the TLC plates with potassium permanganate solution (a mixture of 250 mL H_2O, 2.5 g potassium permanganate, 25 g K_2CO_3, 0.25 g NaOH). For the staining process, the TLC plates were fully submerged into the staining solution, excess of staining reagent was wiped off with cellulose, and the plate was heated up to 300 °C with a heat gun until staining was visibly completed.

Prior to purification by preparative reversed phase (RP) medium-pressure liquid chromatography (MPLC), raw products were dissolved in mixtures of deionized water and methanol (v:v, 4:1) and passed through an syringe filter (regenerated cellulose (RC), 0.45 μM). The used MPLC system was a CombiFlash Rf200 by Teledyne ISCO (Germany), with prepacked columns *FlashPure* (EcoFlex C-18, spherical, 40–60 μm) which were purchased from Buchi (Germany).

Mass spectra were acquired on an Agilent 1260 Infinity II system (Agilent Technologies) consisting of a G7129A autosampler, a G7116A column oven, a G7117C photodiode array detector and a G7111B quaternary pump system. Eluents were directly infused into a QTOF mass spectrometer (Bruker) using an electrospray ionization source which was operated in positive ionization mode. Samples were dissolved in methanol (CH_3OH) at a final concentration of 0.1 mg/mL prior to injection into the HPLC-MS system. The instrument was operated by the Center for Mass Spectrometry (CMS) Team, which is part of the Core Facility of the Department of Chemistry and Chemical Biology at TU Dortmund University.

^{1}H NMR and ^{13}C NMR spectra were acquired using the following NMR instruments: AV 400 Avance III HD NanoBay (400 MHz) (Bruker) DD2 (500 MHz) (Agilent Technologies), AV 500 Avance III HD Prodigy (500 MHz) by *Bruker*, AV 600 Avance III HD CryoProbe (600 MHz) (Bruker), and AV 700 Avance III HD CryoProbe (700 MHz) (Bruker). The instruments were operated by the NMR-Labor Team, which is also part of the Core Facility of the Department of Chemistry and Chemical Biology at TU Dortmund University. NMR data was processed using *MestReNova* x 64 (*v12.0.4*).

General Procedure for Two-Step Headgroup Synthesis

First, sodium hydride (60w% in mineral oil, 1.1 eq.) was added in portions to a solution of alcohol (1 eq.) in dry tetrahydrofuran. Catalytic amounts of 15-crown-5 were added, and the reaction mixture was stirred at 50 °C for 1 hour. Methallyl dichloride (1 eq.) was added slowly, followed by the addition of catalytic amounts of 18-crown-6 and catalytic amounts of potassium iodide. The mixture was continued to stir at 40 °C overnight. After cooling down to room temperature the reaction was quenched with water and the solvent was removed under reduced pressure. The crude product was dissolved in dichloromethane, brine and water and the layers were separated. The aqueous layer was extracted with dichloromethane and the combined organic layers were dried over Na_2SO_4, filtered and the solvent was removed under reduced pressure. Subsequent column chromatography (SiO_2, petrol ether/dichloromethane, *v/v*) yielded the desired monosubstituted intermediate **a***.

Second, sodium hydride (60w% in mineral oil, 1.1 eq.) was added in portions to a solution of alcohol (1 eq.) in dry tetrahydrofuran. Catalytic amounts of 15-crown-5 were added, and the reaction mixture was stirred at 50 °C for 1 hour. The desired monosubstituted intermediate **a*** (1 eq.) was added slowly, followed by the addition of catalytic amounts of 18-crown-6 and catalytic amounts of potassium iodide. The mixture was continued to stir at 70 °C overnight. After cooling to room temperature, the reaction was quenched with water and the solvent was removed under reduced pressure. The crude product was dissolved in dichloromethane, brine and water and the layers were separated. The aqueous layer was extracted with dichloromethane and the combined organic layers were dried over Na_2SO_4, filtered, and the solvent was removed under reduced pressure. Subsequent column chromatography (SiO_2, petrol ether/dichloromethane, *v/v*) led to the desired product **ab** in a good yield over two steps (~50%). Details on possible coupling products, purification conditions, NMR, and MS characterization are provided in the Electronic Supporting Information.

General Procedure for Ozonolysis

The starting material **ab** containing a single double bond (~5 g) was dissolved in dry methanol (35 mL) and dry dichloromethane (35 mL). The mixture was cooled down to −78 °C. The ozone generator Labor-Ozonisator 301.7 (Sander, Germany) was used to obtain an ozone-containing oxygen gas flow (voltage: 7 V, current: 0.3 A, oxygen flow: 1 bar). The ozone-containing oxygen gas flow was passed through the reaction mixture until its color changed to pale blue. Oxygen was then passed through the solution until it became colorless. Sodium borohydride (10 eq.) was added, and the

mixture was stirred and allowed to warm up to room temperature overnight. NH_4Cl (50 mL of a saturated aqueous solution) was added, and the mixture was stirred for 20 minutes. Organic solvent was removed under reduced pressure and the remaining material was suspended in dichloromethane (50 mL), and water (50 mL). The aqueous layer was extracted with dichloromethane (2×40 mL). The combined organic layers were dried over Na_2SO_4, filtered, and the solvent was removed under reduced pressure to obtain the desired product as a colorless oil in high yield (~90%). Details on possible products, NMR, and MS characterization are provided in the Electronic Supporting Information.

General Procedure for Alkylation

Sodium hydride (60w% in mineral oil, 2 eq.) was added in small portions to a solution of asymmetric detergent headgroups containing a single hydroxyl group (1 eq.) in dry *N*,*N*-dimethylformamide. The reaction mixture was stirred at 50 °C for 1 hour. *n*-Bromododecane (2 eq.) was added slowly, and the reaction mixture was stirred at room temperature overnight. The reaction was quenched with water and the solvent was removed under reduced pressure. The crude product was dissolved in dichloromethane, water, brine, and the layers were separated. The aqueous layer was extracted with dichloromethane. The combined organic layers were dried over Na_2SO_4, filtered and the solvent was removed under reduced pressure. Subsequent column chromatography (SiO_2, dichloromethane/ethyl acetate, *v/v*) gave alkylated and fully protected precursors for **1** or **2** in good yields (>80%) as colorless oils. Details on possible coupling products, NMR, and MS characterization are provided in the Electronic Supporting Information.

General Procedure for Debenzylation

To a solution of alkylated and fully protected precursors of **1** or **2** (~4 g) in methanol (10 mL) was added Pd/C (Pd on carbon, 10w% loading, 92.0 mg). The reaction mixture was stirred for 4 days at room temperature under hydrogen atmosphere. The resulting suspension was passed through a syringe filter (0.45 μm, RC) and the solvent was removed under reduced pressure. Subsequent column chromatography (SiO_2, dichloromethane/ ethyl acetate, *v/v*, 1/0→4/1 + 10v% methanol) gave debenzylated detergent precursors **1** or **2** in good yields (>50%) as colorless oils. Details on possible coupling products, NMR, and MS characterization are provided in the Electronic Supporting Information.

General Procedure for Cationic/Non-Ionic Hybrid Detergents

First, to a solution of debenzylated detergent precursors **1** or **2** in toluene was slowly added methanesulfonyl chloride (1.1 eq.) and triethylamine (1.2 eq.). The reaction mixture was stirred at room temperature for 2 hours. The mixture was filtered, washed with toluene, and the solvent in the filtrate was removed under reduced pressure. Subsequent column chromatography (SiO_2, dichloromethane/ethyl acetate, *v/v*) yielded mesylated compounds as colorless oils in good yields (>90%).

Second, mesylated compounds were dissolved in acetonitrile and trimethylamine (4.2 M solution in ethanol, 6 eq.) was added. The reaction mixture was stirred at 50 °C overnight. The solvent was removed under reduced pressure and the crude product was purified by automated column chromatography (RP-C18, water/methanol, 20v%→100v% methanol) to obtain acetal-protected precursors of **1a** or **2a** as white waxy solids in good yields (>70%).

Third, acetal-protected pre-cursors of **1a** or **2a** were dissolved in methanol and catalytic amounts of hydrogen chloride were added. The reaction mixture was stirred at room temperature for 3 hours. The solvent was removed under reduced pressure. The crude product was dissolved in methanol, catalytic amounts of hydrogen chloride were added, and the mixture was stirred at room temperature overnight. The solvent was removed under reduced pressure and the crude product purified by automated column chromatography (RP-C18, water/methanol, 20v%→100v% methanol) to obtain **1a** or **2a** as waxy solids in good yields (>80%). Details on possible coupling products, NMR, and MS characterization are provided in the Electronic Supporting Information for download.

General Procedure for Anionic/Non-Ionic Hybrid Detergents

First, sodium hydride (60w% in mineral oil, 2 eq.) was added in small portions to a solution containing debenzylated detergent precursors **1** or **2** (1 eq.) in dry tetrahydrofuran. The reaction mixture was stirred at 50 °C for 1 hour. Propanesultone (2 eq.) was dissolved in dry tetrahydrofuran, added slowly, and the reaction mixture was stirred at 60 °C overnight under argon atmosphere. The solvent was removed under reduced pressure and the crude product was purified by automated reversed-phase column chromatography (RP-C18, water/methanol, 20v%→100v% methanol) to obtain acetal-protected pre-cursors for **1b** or **2b** in good yields (40–80%) as white waxy solids.

Second, acetal-protected pre-cursors of **1b** or **2b** were dissolved in methanol and catalytic amounts of hydrogen chloride were added. The reaction mixture was stirred at room temperature for 3 hours. The solvent was removed under reduced pressure. The crude product was dissolved in methanol, catalytic amounts of hydrogen chloride were added, and the mixture was stirred at room temperature overnight. The solvent was removed under reduced pressure and the crude product purified by automated column chromatography (RP-C18, water/methanol, 20v%→100v% methanol) to obtain **1b** or **2b** as waxy solids in good yields (>80%). Details on NMR, and MS characterization are provided in the Electronic Supporting Information.

Modular Chemistry of Hydroxyl Group

In addition to the preparation of ionic/non-ionic hybrid detergents (**1a**, **2a**, **1b**, **2b**), we explored the modular chemistry of the single hydroxyl group in debenzylated detergent precursors **1** or **2**. Specifically, the single hydroxyl group could be converted into an azide,[11] amine,[11] bromine,[16] or propargylated,[17] using previously established procedures. Details on reaction and purification conditions, NMR, and MS characterization are provided in the Electronic Supporting Information.

Relative Molecular Weight of Headgroup

To estimate the relative ionic character of hybrid detergents (**1a**, **2a**, **1b**, **2b**), the molecular weight of the ionic group was divided by the total molecular weight of the headgroup. In the cases of DTAB and SDS, the molecular weight of the ionic group is equal to the total molecular weight of the headgroup. Lower relative molecular weights were obtained in the cases of ionic/non-ionic hybrid detergents as shown in Figure 2C.

Conductivity

For conductivity measurements, detergent solutions were prepared in deionized water at 2x cmc. All samples were passed through a

syringe filter (0.22 μm, RC) and equilibrated for 16 hours at room temperature (approximately 22 °C) prior analysis. The samples were analyzed in disposable folded capillary cells (DTS 1070), using a Zetasizer Nano-ZS ZEN3600 instrument (Malvern, UK). Utilized instrumental parameters were adopted from Morris *et al.* as follows:[50] measurement type (zeta potential), material (polystyrene latex), dispersant (water), model (Smoluchowski), sample viscosity parameters (use dispersant viscosity as sample viscosity), temperature (22.5 °C), equilibration time (120 s), cell type (disposable folded capillary cells, DTS 1070), measurement duration (manual), number of runs (30), number of measurements (3), delay between the measurements (300 s), measurement settings (automatic attenuation selection, automatic voltage selection), data processing (auto mode). SDS (≥99%) and DTAB (99%) were used as supplied. All other detergents were synthesized as described above.

Critical Micelle Concentration

To determine critical micelle concentration (cmc) values, we utilized a previously established protocol.[51] Briefly, dilution series with detergent concentrations between 10^{-8} and 20 mg·mL^{-1} were prepared in ultrapure water, which was obtained from a Milli-Q system (18.2 MΩ·cm). All samples were filtered (0.22 μm, RC) and equilibrated for at least for 16 hours at room temperature (approximately 22 °C) prior analysis. The samples were analyzed in cuvettes (Quartz Suprasil, width x length: 2 mm×10 mm) using a Zetasizer Nano-ZS ZEN3600 (Malvern, UK). The instrumental parameters were as follows: measurement type (size), material (polystyrene latex), dispersant (water), sample viscosity parameters (use dispersant viscosity as sample viscosity), temperature (22.5 °C), equilibration time (120 s), cell type (quartz cuvettes), measurement angle (173° backscatter), measurement duration (manual), number of runs (11), run duration (10 s), number of measurements (3), delay between the measurements (0 s), data processing (general purpose, normal resolution).

To determine cmc values, the diffusion coefficient related to the most abundant particle size distribution at each concentration was extracted from the Zetasizer measurement data and plotted against the detergent concentration. The logarithm of the diffusion coefficient was plotted against the logarithm of the detergent concentration. The double logarithmic plots showed two characteristic regions. (1) A flat region with smaller diffusion coefficients at lower detergent concentrations which are like values obtained from pure deionized water. (2) Consistently larger diffusion coefficients at higher concentrations which are different to those obtained in pure deionized water. The concentration that marks the transition between both regions (1)–(2) was taken as the cmc value (Figure S4). The cmc data are summarized in Figure 2A–B in the manuscript and Table S1 in the Supporting Information. To validate our utilized cmc determination method, we successfully reproduced cmc values of SDS (≥99%)[52] and DTAB (99%).[53]

Cryo-Electron Microscopy

For Cryo-EM analysis of micelles, **1a**, **1b**, **2a** and **2b** were dissolved in water to obtain a final concentration of approximately 6x cmc. An aliquot (4 μL) of each sample was applied to freshly glow-discharged UltrAuFoil 1.2/1.3 holey-gold grids (Quantifoil). Excess liquid was removed by blotting and grids were vitrified by rapid plunging into liquid ethane. Data were recorded on a Talos Arctica microscope (Thermo Fisher Scientific) equipped with a Falcon III direct electron detector (Thermo Fisher Scientific) in linear mode. A total electron exposure of 56.5 e/Å2 was distributed over 40 frames. The nominal magnification was 120,000, resulting in a pixel size of 1.21 Å/px. Micrographs were recorded using a volta phase plate at a set defocus of −1.2 μm. Micrograph movies were motion corrected and frames merged using MotionCor2[54] and motion corrected micrographs subsequently filtered using a 10 px median filter and contrast-enhanced in FIJI.[55] Representative cryo-EM data are shown in Figure 2B in the manuscript and Figure S1 in the Supporting Information.

Probing Micellar Polarity Surrounding Guest Molecules

To estimate the polarity of the micellar environment surrounding solubilized guest molecules in aqueous detergent solutions, a previously established procedure was adopted from Kurniasih *et al.*[31] Briefly, detergent stock solutions were prepared in deionized water at 6x cmc. A stock solution of Nile Red, dipyridamole, and doxorubicin with a concentration of 1 mg/mL was prepared in methanol. For every detergent-dye combination, a 10 μL aliquot of the chosen dye stock solution was added to 1 mL of each detergent solution and a UV-Vis spectrum was recorded after an equilibration time of 20 hours at room temperature (~22 °C) using quartz cuvettes. To compare changes in polarity of the environment surrounding the solubilized guest, the absorption maxima were extracted from spectral data. The lower the wavelength of the absorption maximum, the lower the polarity of the environment surrounding the solubilized dye Nile Red under the experimental conditions employed.[31] Spectra obtained from dipyridamole and doxorubicin were analyzed following the same assumption. Wavelength positions of absorption maxima of Nile Red are summarized in Figure 2D and 2E in the manuscript and UV-Vis data of other guest molecules are shown in Figure S2.

Encapsulation Studies

To study the detergents' solubilization efficiencies, a procedure was adopted from Thota *et al.*[35] A stock solution of Nile Red (0.5 mg/mL) or dipyridamole (0.5 mg/mL) was prepared in THF. A thin film of the dye or drug was prepared by adding 1 mL of the stock solution to an Eppendorf tube and leaving it open in a fume hood for 72 hours to let the solvent evaporate. Afterwards 1 mL of an aqueous detergent solution at 2x cmc was added to each tube and the mixture was shaken with 500 rpm at 22 °C for 16 hours in the case of Nile Red samples and three hours in the cases of dipyridamole samples. The supernatant was separated by centrifugation (20000 g, 5 minutes, 22 °C) and filtered through a syringe filter (0.2 μm, RC) to remove remaining bits of solid Nile Red or dipyridamole. As a negative control, deionized water was used to resolubilize Nile Red or dipyridamole instead of amphiphilic solution and the sample was handled as described above. To determine the relative amounts of solubilized Nile Red or dipyridamole, 400 μL of each supernatant was dried for 48 hours in the cases of Nile Red and 24 hours in the cases of dipyridamole using a speed vacuum concentrator (rotation speed: 1360 rpm). Subsequently, the dry pellets were resolubilized in 500 μL of DMSO. The absorbance values were determined at a wavelength of 552 nm for Nile Red and 416 nm for dipyridamole. The concentrations and molar amounts of solubilized Nile Red or dipyridamole were calculated by means of the extinction coefficients of Nile Red [$\varepsilon_{552,DMSO} = (37500 \pm 4900) M^{-1} \cdot cm^{-1}$] or dipyridamole [$\varepsilon_{416,DMSO} = (12400 \pm 5257) M^{-1} \cdot cm^{-1}$]. To determine the solubilization efficiency, molar amounts of solubilized Nile Red or dipyridamole were divided by the molar amounts of utilized detergents. Data are shown in Figure 3A and Figure S3 with standard deviation (±SD) from three independent repeats (n = 3).

Hard Water Tolerance

To determine resistance against precipitation in hard water, a procedure was adopted from Rodriguez *et al.*[56] Stock solutions of $CaCl_2$ and $MgCl_2$ (2 M) were prepared and filtered through a syringe filter (0.2 μm, RC). Serial dilutions were prepared for each detergent with concentrations ranging from $2 \cdot 10^{-5}$ M to 2 M. An aliquot from each concentration (500 μL) was mixed with an aliquot of an aqueous detergent solution at 4x cmc (500 μL). Subsequently, the samples were stored in the fridge for 24 hours and then stored at room temperature (~22 °C) for 72 hours. To track sample precipitation, samples were transferred into quartz cuvettes and absorbance values at 500 nm were measured using a NanoPhotometer (Implen). To visualize differences in hard water tolerance, absorbance values at 500 nm were plotted against the ion concentration (Figure 3B). SDS (≥95%) and DTAB (99%) were used as supplied. All other detergents were synthesized as described above.

Minimal Inhibitory Concentration

To determine minimal inhibitory concentration (MIC) values of detergents, a procedure was adopted from Wiegand *et al.*[45] For preparation of sterile agar plates, a mixture of agar-agar (1.7 g), Müller Hinton Broth medium (MH medium) (2.1 g), and deionized water (100 mL) was autoclaved, poured into sterile petri dishes, and allowed to solidify at room temperature. For the preparation of individual bacterial colonies, a mixture of MH medium (4.2 g) and deionized water (200 mL) was autoclaved. A glycerol stock solution of *E. coli* MG1655 (750 μL) was dissolved in 5 mL sterile MH-medium and incubated for 3.5 hours at 37 °C. Different dilutions were prepared from the incubated suspension (1:500&1:1000&1:10000). From each dilution, a 50 μL aliquot was pipetted onto a sterile agar plate. The suspensions were spread with a sterile L-shaped cell spreader and the agar plates were incubated at 37 °C for 16 hours to obtain individual colonies.

To determine MIC values of detergents, detergent stock solutions were prepared in sterile MH medium. Furthermore, a single colony was transferred into 5 mL sterile MH medium. The mixture was shaken at 37 °C with 180 rpm. After 3.5 hours the optical density at 600 nm of the suspension was determined using disposable cuvettes and a NanoPhotometer (Implen). Bacterial suspension was diluted with sterile MH broth to a concentration of 1×10^8 cfu/mL (OD600 = 0.06). A 1:100 dilution was created in sterile MH broth to prepare the inoculum for the MIC test.

An automatic 8-channel pipette from Eppendorf (Eppendorf Research plus 1200 μL) was used to pipette sterile MH medium (100 μL) into the wells 1–10 and 12 (growth control) of a sterile 96-well plate. For a sterile control, MH-medium (200 μL) was pipetted into the 11th well. Next, detergent stock solution (100 μL) was added to the first well and the solution was mixed by pipetting seven times up and down. Then 100 μL of the solution in the first well was transferred to the second well and mixed again as described for the first well before. This procedure was repeated until reaching the 10th well. No detergent was added to the 11th and 12th well. Subsequently, *E. coli* inoculum (100 μL) was added to the wells 1–10 and 12. The 96-well plate was incubated at 37 °C overnight. The lowest detergent concentration at which no visible bacterial growth occurred was taken as MIC (Table 1).[45] SDS (≥95%) and DTAB (99%) were used as supplied. All other detergents were synthesized as described above.

Cell Viability Analysis

To determine the effect of detergents in cell viability, HaCaT cells were plated into white 384-well cell culture plates (Greiner Bio-One) using a Multidrop™ reagent dispenser (Thermo) at 800 cells per well to ensure linear and optimal luminescent signal intensity (A431: 150 cells/well; A375: 100 cells/well; SK-Mel-5: 200 cells/well; HaCaT: 800 cells/well). Following incubation for 24 h in a humidified atmosphere at 37 °C/5% CO_2, cells were treated with detergents in serial dilutions ranging from 10000 μM down to 0.6 μM for SDS, **1b**, **2b**; from 1000 μM to 0.06 μM for [G1] OGD, **1a**, **2a**; and for DTAB from 0.07 μM to 1160 μM using an Echo 650 acoustic liquid handler (Beckman Coulter).

Cell viability was analyzed on day 5 using the CellTiter-Glo® assay (Promega) as per manufacturer's instructions. Luminescence was recorded using an EnVision Multilabel 2104 Plate Reader (PerkinElmer) using 500 ms integration time. The obtained data were normalized to the plate positive control (30 μM staurosporine) and negative control (ddH_2O) and subsequently analyzed and fitted with the Quattro Software Suite (Quattro Research) using a four-parameter logistic model. As quality control, the Z′-factor was calculated from 16 positive and negative control values. Only assay results showing a Z′-factor ≥0.5 were used for further analysis. All experimental points were measured in technical duplicates for each plate and were replicated in at least three biologically independent experiments. SDS (≥95%) and DTAB (99%) were used as supplied. All other detergents were synthesized as described above.

Author Contributions

V. Wycisk and L. H. Urner conceptualized the work. V. Wycisk, J. S. Behnke, M. Binsch, and M.-C. Wagner established the modular two-step synthesis of hybrid detergents. L. Nielinger established the cmc, solubilization efficiency, and hard-water tolerance of hybrid detergents. M. Seewald and J. Weisner established the cell compatibility of hybrid detergents. T. Raisch established the cryo-EM characterization of hybrid detergents. The manuscript was written by L. H. Urner with input from all authors.

Acknowledgements

The Ministry of Culture and Science of the German State of North Rhine-Westphalia (NRW return program grant) and the Fonds der Chemischen Industrie (Material Cost Allowance) are gratefully acknowledged for providing financial support. This work was also supported by the "Netzwerke 2021" program, an initiative of the Ministry of Culture and Science of the State of North Rhine-Westphalia (CANcerTARgeting, NW21-062C). Prof. Daniel Rauh and Prof. Herbert Waldmann are gratefully acknowledged for providing the lab infrastructure required for cellular assays and ozonolysis, respectively. The Core Facility of the TU Dortmund University is gratefully acknowledged for continuous support in compound characterization. Open Access funding enabled and organized by Projekt DEAL.

Conflict of Interests

The authors declare no conflict of interest.

Data Availability Statement

Datasets supporting this article have been uploaded as part of the Electronic Supporting Information.

Keywords: detergent · micelle · cell toxicity · modular chemistry · supramolecular chemistry

[1] a) A. C. Kogawa, B. G. Cernic, L. G. Domingos do Couto, H. R. N. Salgado, *Saudi Pharm. J.* **2017**, *25*, 934–938; b) H. J. Lee, H. S. Lee, T. Youn, B. Byrne, P. S. Chae, *Chem* **2022**, *8*, 980–1013; c) S. Mohapatra, L. Yutao, S. G. Goh, C. Ng, Y. Luhua, N. H. Tran, K. Y.-H. Gin, *J. Hazard. Mater.* **2023**, *445*, 130393; d) J. M. Boyce, *Antimicrob. Resist. Infect. Control* **2023**, *12*, 32; e) J. R. G. Asio, J. S. Garcia, C. Antonatos, J. B. Sevilla-Nastor, L. C. Trinidad, *Emerging Contaminants* **2023**, *9*, 100205; f) V. Wycisk, M.-C. Wagner, L. H. Urner, *ChemPlusChem* **2023**, e202300386; g) V. S. Nagtode, C. Cardoza, H. K. A. Yasin, S. N. Mali, S. M. Tambe, P. Roy, K. Singh, A. Goel, P. D. Amin, B. R. Thorat, J. N. Cruz, A. P. Pratap, *ACS Omega* **2023**, *13*, 11674–11699.
[2] K. C. Cheng, Z. S. Khoo, N. W. Lo, W. J. Tan, N. G. Chemmangattuvalappil, *Heliyon* **2020**, *6*, e03861.
[3] L. H. Urner, A. Ariamajd, A. Weikum, *Chem. Sci.* **2022**, *13*, 10299–10307.
[4] M. Seewald, L. Nielinger, K. Alker, J.-S. Behnke, V. Wycisk, L. H. Urner, *Angew. Chem. Int. Ed.* **2024**, https://doi.org/10.1002/ange.202403833.
[5] a) F. Malek, E. Ranjbari, M. Mirmohammadkhani, D. Pahlevan, *J. Occup. Med. Toxicol.* **2022**, *17*, 6; b) G. F. Nieman, C. E. Bredenberg, *J. Appl. Physiol.* **1985**, 129–136; c) K. Saito, K. Orimo, T. Kubo, M. Tamari, A. Yamada, K. Motomura, H. Sugiyama, R. Matsuoka, N. Nagano, Y. Hayashi, K. Arae, M. Hara, M. Ikutani, T. Fukuie, K. Sudo, A. Matsuda, Y. Ohya, S. Fujieda, H. Saito, S. Nakae, K. Matsumoto, A. C. Akdis, H. Morita, *Allergy* **2023**, *78*, 1878–1892; d) I. Ogulur, Y. Pat, T. Aydin, D. Yazici, B. Rückert, Y. Peng, J. Kim, U. Radzikowska, P. Westermann, M. Sokolowska, R. Dhir, M. Akdis, K. Nadeau, C. A. Akdis, *J. Allergy Clin. Immunol.* **2023**, *151*, 469–484; e) K. R. Harrison, A. D. Kappell, P. J. McNamara, *Environ. Pollut.* **2020**, *257*, 113472; f) R. Lucassen, N. van Leuven, D. Bockmühl, *Microorganisms* **2024**, *12*, 712.
[6] Â. S. Inácio, K. A. Mesquita, M. Baptista, J. Ramalho-Santos, W. L. C. Vaz, O. V. Vieira, *PLoS One* **2011**, *6*, e19850.
[7] F. G. Jarvis, M. J. HJohnson, *J. Am. Chem. Soc.* **1949**, *71*, 4124–4126.
[8] K.-A. Nguyen, M. Peuchmaur, S. Magnard, R. Haudecoeur, C. Boyère, S. Mounien, I. Benammar, V. Zampieri, S. Igonet, V. Chaptal, A. Jawhari, A. Boumendjel, P. Falson, *Angew. Chem. Int. Ed.* **2018**, *57*, 2948–2952.
[9] G. Viscardi, P. Quagliotto, C. Barolo, P. Savarino, E. Barni, E. Fisicaro, *J. Org. Chem.* **2000**, *65*, 8197–8203.
[10] P. Quagliotto, G. Viscardi, C. Barolo, D. D'Angelo, E. Barni, C. Compari, E. Duce, E. Fisicaro, *J. Org. Chem.* **2005**, *70*, 9857–9866.
[11] M. Wyszogrodzka, R. Haag, *Chem. Eur. J.* **2008**, *14*, 9202–9214.
[12] L. H. Urner, K. Goltsche, M. Selent, I. Liko, M.-P. Schweder, C. V. Robinson, K. Pagel, R. Haag, *Chem. Eur. J.* **2021**, *27*, 2537–2542.
[13] a) D. R. Boyd, M. A. Mckervey, *Q. Rev. Chem. Soc.* **1968**, *22*, 95–122; b) M. Ghosh, V. S. Shinde, M. Rueping, *Beilstein J. Org. Chem.* **2019**, *15*, 2710–2746; c) D. J. Ramón, M. Yus, *Angew. Chem. Int. Ed.* **2005**, *44*, 1602–1634; d) X. Zhang, F. Wang, C.-H. Tan, *JACS Au* **2023**, *3*, 700–714.
[14] a) J.-F. Lutz, H. Schlaad, *Polymer* **2008**, *49*; b) V. Percec, P. Leowanawat, H.-J. Sun, O. Kulikov, C. D. Nusbaum, T. M. Tran, A. Bertin, D. A. Wilson, M. Peterca, S. Zhang, N. P. Kamat, K. Vargo, D. Moock, E. D. Johnston, D. A. Hammer, D. J. Pochan, Y. Chen, Y. M. Chabre, T. C. Shiao, M. Bergeron-Brlek, S. André, R. Roy, H.-J. Gabius, P. A. Heiney, *J. Am. Chem. Soc.* **2013**, *135*, 9055–9077; c) L. H. Urner, I. Liko, H.-Y. Yen, K. K. Hoi, J. R. Bolla, J. Gault, F. G. Almeida, M.-P. Schweder, D. Shutin, S. Ehrmann, R. Haag, C. V. Robinson, K. Pagel, *Nat. Commun.* **2020**, *11*, 564.
[15] B. N. S. Thota, L. H. Urner, R. Haag, *Chem. Rev.* **2015**, *116*, 2079–2102.
[16] T. W. Baughman, J. C. Sworen, K. B. Wagener, *Tetrahedron* **2004**, *60*, 10943–10948.
[17] L. H. Urner, B. Schade, M. Schulze, K. Folmert, R. Haag, K. Pagel, *ChemPhysChem* **2019**, *20*, 1690–1697.
[18] V. Wycisk, K. Achazi, P. Hillmann, O. Hirsch, C. Kuehne, J. Dernedde, R. Haag, K. Licha, *ACS Omega* **2016**, *1*, 808–817.
[19] a) J. N. Israelachvili, D. J. Mitchell, B. W. Ninham, *J. Chem. Soc. Faraday Trans. 2* **1976**, *72*, 1525–1568; b) Y. Lu, E. Zhang, J. Yang, Z. Cao, *Nano Res.* **2018**, *11*, 4985–4998; c) H. S. Wang, W. Ran, W. Zhang, W. Dai, H. Wang, C. F. Anderson, Z. Wang, C. Zheng, P. Zhang, Y. Li, H. Cui, *PNAS* **2020**, *117*, 4518–4526; d) J.-S. Behnke, L. H. Urner, *Anal. Bioanal. Chem.* **2023**, *415*, 3897–3909.
[20] a) K. A. Sharp, *Curr. Opin. Struct. Biol.* **1994**, *4*, 234–239; b) B. H. Honig, W. L. Hubbell, R. F. Flewelling, *Ann. Rev. Biophys. Chem.* **1986**, *15*, 163–193; c) M. Ballauff, *RSC Adv.* **2022**, *12*, 10105–10113; d) D. Lauster, K. Osterrieder, R. Haag, M. Ballauff, A. Herrmann, *Front. Microbiol.* **2023**, *14*, 1169547.
[21] A. S. Rafique, S. Khodaparast, A. S. Poulos, W. N. Sharratt, E. S. J. Robles, J. T. Cabral, *Soft Matter* **2020**, *16*, 7835–7844.
[22] a) M. Pisárčik, F. Devínsky, M. Pupák, *Open Chemistry* **2015**, *13*, 922–931; b) A. Jusufi, A.-P. Hynninen, M. Haataja, A. Z. Panagiotopoulos, *J. Phys. Chem. B.* **2009**, *113*, 6314–6320.
[23] W. Luo, M. Yang, Y. Zhao, H. Wang, X. Yang, W. Zhang, F. Thao, S. Zhao, H. Tao, *Chem. Eur. J.* **2022**, *28*, e202202242.
[24] F. Legrand, C. Breyton, P. Guillet, C. Ebel, G. Durand, *J. Org. Chem.* **2016**, *81*, 681–688.
[25] A. E. Speers, C. C. Wu, *Chem. Rev.* **2007**, *107*, 3687–3714.
[26] a) G. G. Prive', *Methods* **2007**, *41*, 388–397; b) N. T. Johansen, F. G. Tidemand, M. C. Pedersen, L. Arleth, *Biochimie* **2023**, *205*, 3–26; c) L. H. Urner, *Curr. Opin. Chem. Biol.* **2022**, *69*, 102157.
[27] a) D. Abooali, R. Soleimani, *Sci. Rep.* **2023**, *13*, 13361; b) A. Khalfallah, S. Mazzouzi, *J. Surfactants Deterg.* **2020**, *24*, 193–198.
[28] J. M. Corkill, J. F. Goodman, J. R. Tate, *Trans. Faraday Soc.* **1964**, *60*, 986–995.
[29] M. E. Hobbs, *J. Phys. Chem.* **1951**, *55*, 675–683.
[30] A. R. Tehrani-Bagha, K. Holmberg, *Materials* **2013**, *6*, 580–608.
[31] I. N. Kurniasih, H. Liang, P. C. Mohr, G. Khot, J. P. Rabe, A. Mohr, *Langmuir* **2015**, *31*, 2639–2648.
[32] A. Ray, S. Das, N. Chattopadhyay, *ACS Omega* **2019**, *4*, 15–24.
[33] W. Teo, A. V. Caprariello, M. L. Morgan, A. Luchicchi, G. J. Schenk, J. T. Joseph, J. J. G. Geurts, P. K. Stys, *PNAS* **2021**, *118*, e2016897118.
[34] a) I. E. Borissevitch, C. P. F. Borges, G. P. Borissevitch, V. E. Yushmanov, S. R. W. Louro, M. Tabak, *Z. Naturforsch.* **1996**, *51c*, 578–590; b) A. Banerjee, D. Mukherjee, A. Bera, R. Ghosh, S. Mondal, S. Mukhopadhyay, R. Das, H. M. Altass, S. S. A. Natto, Z. Moussa, S. A. Ahmed, A. Chattopadhyay, S. K. Pal, *Sci. Rep.* **2022**, *12*, 18881; c) Z. Vinarov, V. Katev, D. Radeva, S. Tcholakova, N. D. Denkov, *Drug Dev. Ind. Pharm.* **2017**, *44*, 677–686.
[35] B. N. S. Thota, H. v. Berlepsch, C. Böttcher, R. Haag, *Chem. Commun.* **2015**, *51*, 8648–8651.
[36] P. A. Bhat, A. A. Dar, G. M. Rather, *J. Chem. Eng. Data* **2008**, *53*, 1271–1277.
[37] C. G. Wermuth, in *The Practice of Medicinal Chemistry (Second Edition)* (Ed.: C. G. Wermuth), Academic Press, London, **2003**, pp. xiii-xiv.
[38] D. Bajpai, V. K. Tyagi, *J. Oleo Sci.* **2007**, *56*, 327–340.
[39] T. Odahara, K. Odahara, *Heliyon* **2018**, *4*, E01073.
[40] a) K. Gotoh, K. Horibe, Y. Mei, T. Tsujisaka, *J. Oleo Sci.* **2016**, *65*, 123–133; b) C. H. Rodriguez, L. H. Lowery, J. F. Scamehorn, J. H. Harwell, *J. Surfactants Deterg.* **2001**, *4*, 1–14; c) G. Dass, M. S. Revathy, P. Manorama, A. Kumar, Ramesh, *J. Environ. Nanotechnol.* **2019**, *8*, 23–25.
[41] T. Lam, Y. Liu, F. Iuchi, Y. Huang, K. Du, Y. Dai, J. Wu, L. Lim, J. Goo, Y. Ishida, J. Liu, J. Xu, *iMeta* **2023**, *2*, e110.
[42] a) A. Ramata-Stunda, M. Boroduskis, V. Vorobjeva, J. Ancans, *EEB* **2013**, *11*, 159–177; b) N. A. Falk, *J. Surfactants Deterg.* **2019**, *22*, 1119–1127.
[43] a) M. A. Liebert, *J. Am. Coll. Toxicol.* **1983**, *2*, 127–181; b) Y. Takagi, M. Shimizu, Y. Morokuma, M. Miyaki, A. Kiba, K. Matsuo, K. Isoda, H. Mizutani, *Int. J. Cosmet. Sci.* **2014**, *36*, 305–311.
[44] E. Soupene, W. C. van Heeswijk, J. Plumbridge, V. Stewart, D. Bertenthal, H. J. Lee, G. Prasad, O. Paliy, P. Charernnoppakul, S. Kusti, *J. Bacteriol.* **2003**, *185*, 5611–5626.
[45] I. Wiegand, K. Hilpert, R. E. W. Hancock, *Nat. Protoc.* **2008**, *3*, 163–175.
[46] a) S. Halder, K. K. Kumar, R. Sarkar, S. Mukherjee, P. Saha, S. Haldar, S. Karmakar, T. Sen, *SpingerPlus* **2015**, *4*, 672; b) S. Eisenberg, E. Haimov, G. F. W. Walpole, J. Plumb, M. M. Kozlov, S. Grinstein, *Mol. Biol. Cell.* **2021**, *32*, 211–310.

[47] a) U. Kragh-Hansen, M. le Maire, J.-P. Noel, T. Gulik-Krzywicki, J. V. Moller, *Biochemistry* **1993**, *32*, 1648–1656; b) S. Vaidyanathan, B. G. Orr, M. M. B. Holl, *J. Phys. Chem. B.* **2014**, *118*, 2112–2123.
[48] F. Costamagna, H. Hillaireau, J. Vergnaud, D. Clarisse, L. Jamgotchian, O. Loreau, S. Denis, E. Gravel, E. Doris, E. Fattal, *Nanoscale* **2020**, *12*, 2452–2463.
[49] L. H. Urner, F. Fiorentino, D. Shutin, J. B. Sauer, M. T. Agasid, T. J. El-Baba, J. R. Bolla, P. J. Stansfeld, C. V. Robinson, *J. Am. Chem. Soc.* **2024**, https://doi.org/10.1021/jacs.1023c14358.
[50] S. A. V. Morris, R. T. Thompson, R. W. Glenn, K. P. Ananthapadmanabhan, G. B. Kasting, *Int. J. Cosmet. Sci.* **2019**, *41*, 55–56.
[51] V. P. Arkhipov, R. V. Arkhipov, E. V. Petrova, A. Filippov, *Magn. Reson. Chem.* **2023**, *61*, 345–355.
[52] S. G. Oh, D. O. Shah, *Langmuir* **1991**, *7*, 1316–1318.
[53] A. Ali, S. Uzair, N. A. Malik, M. Ali, *J. Mol. Liq.* **2014**, *196*, 395–403.
[54] S. Q. Zheng, E. Palovcak, J.-P. Armache, K. A. Verba, Y. Cheng, D. A. Agard, *Nat. Methods* **2017**, *14*, 331–332.
[55] J. Schindelin, I. Arganda-Carreras, E. Frise, V. Kaynig, M. Longair, T. Pietzsch, S. Preibisch, C. Rueden, S. Saalfeld, B. Schmid, J.-Y. Tinevez, D. J. White, V. Hartenstein, K. Eliceiri, P. Tomancak, A. Cardona, *Nat. Methods* **2012**, *9*, 676–682.
[56] C. H. Rodriguez, L. H. Lowery, J. F. Scamehorn, J. H. Harwell, *J. Surfactants Deterg.* **2001**, *4*, 1–14.

Manuscript received: May 10, 2024
Accepted manuscript online: May 31, 2024
Version of record online: July 15, 2024